LBL-14874
Preprint c.2

Lawrence Berkeley Laboratory
UNIVERSITY OF CALIFORNIA

Accelerator & Fusion Research Division

RECEIVED
LAWRENCE
BERKELEY LABORATORY
JUL 5 1983
LIBRARY AND
DOCUMENTS SECTION

Submitted to Physical Review A

MEASUREMENTS OF INELASTIC COLLISIONS BETWEEN Cs^+ IONS BY A PLASMA TARGET TECHNIQUE

K.R. Stalder, K.H. Berkner, and R.V. Pyle

May 1983

TWO-WEEK LOAN COPY
This is a Library Circulating Copy which may be borrowed for two weeks. For a personal retention copy, call Tech. Info. Division, Ext. 6782.

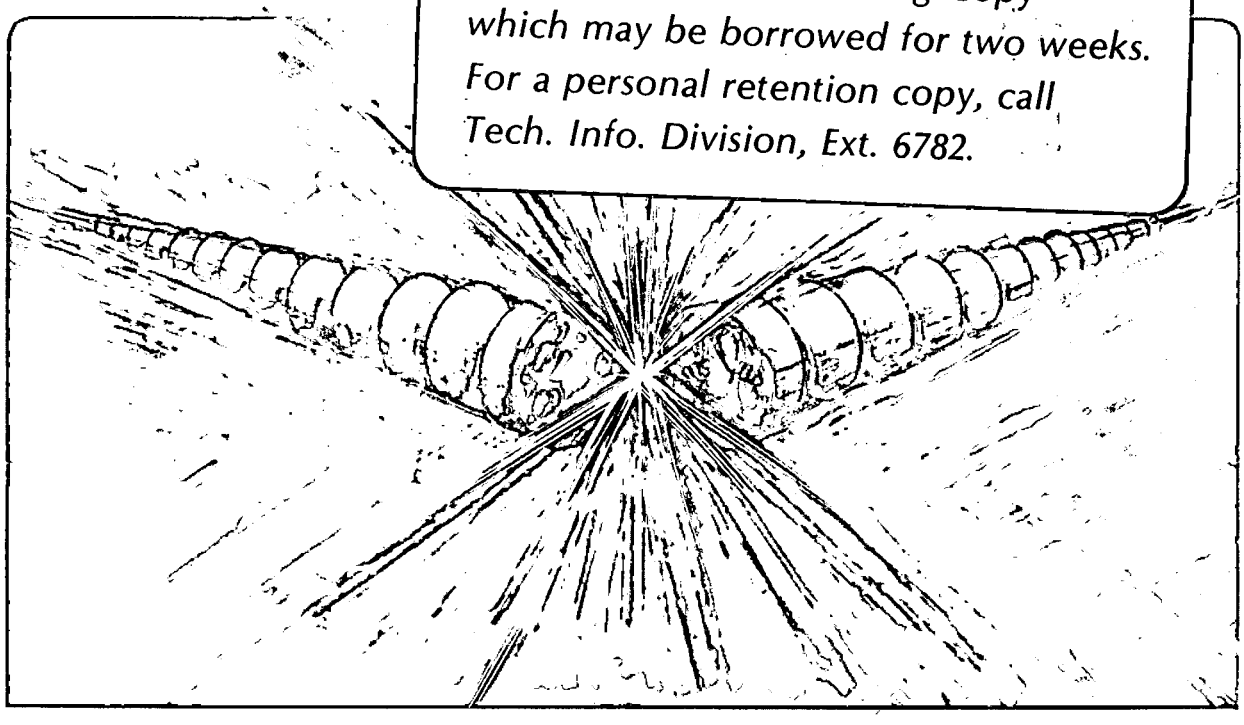

LBL-14874 c.2

Prepared for the U.S. Department of Energy under Contract DE-AC03-76SF00098

DISCLAIMER

This document was prepared as an account of work sponsored by the United States Government. While this document is believed to contain correct information, neither the United States Government nor any agency thereof, nor the Regents of the University of California, nor any of their employees, makes any warranty, express or implied, or assumes any legal responsibility for the accuracy, completeness, or usefulness of any information, apparatus, product, or process disclosed, or represents that its use would not infringe privately owned rights. Reference herein to any specific commercial product, process, or service by its trade name, trademark, manufacturer, or otherwise, does not necessarily constitute or imply its endorsement, recommendation, or favoring by the United States Government or any agency thereof, or the Regents of the University of California. The views and opinions of authors expressed herein do not necessarily state or reflect those of the United States Government or any agency thereof or the Regents of the University of California.

LBL-14874

Measurements of Inelastic Collisions between Cs^+ Ions by a Plasma Target Technique*

K. R. Stalder†, K. H. Berkner and R. V. Pyle

Lawrence Berkeley Laboratory
University of California
Berkeley, CA 94720

Received

Abstract

Cross sections for Cs^{++} formation in $Cs^+ + Cs^+$ collisions have been measured by a plasma target technique for center of mass energies from 50 to 110 keV. The measured cross sections for the sum of ionization and charge exchange are in moderate agreement with the results of Peart et al., and disagree with the results of Dunn et al. and Neill et al. at the lower energies. The experimental technique and possible sources of error are discussed in light of the discrepancy between the results of the three groups.

---

* This work was supported, in part by a grant from the Director's Program Development Fund, Lawrence Berkeley Laboratory, and by the Director, Office of Fusion Energy, Applied Plasma Physics Division of the U.S. Department of Energy under Contract No. DE-AC03-76SF00098.

† Present address: Physics Department; University of California, Irvine, CA 94717.

I. Introduction

Cross sections for charge-changing collisions between heavy ions are relevant to proposed heavy-ion fusion schemes requiring storage rings to accumulate the required beam intensity. The loss of ions by collisions not only limits the beam intensity that can be achieved, but also may cause damage to the storage ring walls. These problems have been discussed previously in detail in workshops on heavy ion fusion.[1] Cs^+ is a candidate for a heavy-ion-fusion driver since it has a relatively large Z and a closed shell electronic configuration. Previous experimental work on Cs^+-Cs^+ collisions, with crossed ion beams, has been reported by Dunn et al.[2] and Peart et al.[3,4]; recently, a more thorough investigation of the experiment by Dunn et al.[2] has been reported by Neill et al.[5] Olson and Liu[6] have reported a theoretical estimate for the Cs^+-Cs^+ process, but the precision of the theory is not great enough to directly compare with experiments.

In this paper we present cross-section measurements for Cs^+-Cs^+ collisions by using a cesium plasma as a target for a cesium ion beam.[7] The beam is passed through the plasma, and collisions resulting in formation of Cs^{++} ions in the beam are detected with a secondary emission detector. The Cs^{++} fraction of the beam, measured as a function of plasma line density, yields a cross section for Cs^{++} formation by either of the following two reactions:

$$Cs^+ + Cs^+ \rightarrow Cs^+ + Cs^{++} + e$$

$$Cs^+ + Cs^+ \rightarrow Cs^0 + Cs^{++}$$

Results for collisions of other alkali metal ions also have been reported by Peart et al.[8] Experimental work on the electronically similar, yet experimentally simpler, Cs^+ + Xe system has been reported by Tanis et al.[9], Flaks et al.[10], Ogurtsov et al.[11], and more recently by Neill et al.[5].

The experimental results for the Cs^+ - Cs^+ system have tended to disagree, even in the energy dependence, for the two measurements done by the crossed beam technique. In this paper we present Cs^+ - Cs^+ cross-section results obtained with the plasma target technique.

II. Apparatus and Description of the Technique

A. Overview

The experimental configuration is shown in Fig. 1. A beam of Cs^+ ions was formed by a beta-eucryptite thermionic type ion source in the dome of a 250 kV accelerator. The beam was focused, then momentum analyzed in a bending magnet and collimated by two apertures C_1 and C_2 shown in Fig. 1. The beam then entered the target chamber and crossed the plasma where charge changing collisions occurred. The product beams were separated by the magnetic field which confined the plasma and entered a separate analysis chamber for detection. The primary Cs^+ beam was detected with a Faraday cup and the Cs^{++} beam was detected with a secondary emission detector. Data were collected and analyzed by an on-line computer system.

B. Plasma Target

The plasma target, known in the plasma literature as a Q machine and shown in Fig. 2, was created by using a hot tungsten plate to

thermally ionize a spray of cesium atoms from an oven directed at the hot plate. The hot plate was heated by electron bombardment from a lanthanum hexaboride cathode which was heated radiatively from the tungsten hot plate.[12] The hot plate temperature, approximately 2800 K, resulted in enough thermionic electron emission to neutralize the plasma. The plasma was confined radially by a magnetic field; axially the plasma drifted along the magnetic field lines and was collected on a grounded cold plate.

A jacket cooled with the exhaust from a liquid nitrogen reservoir surrounded the plasma target chamber. This lowered the wall temperature to approximately -120°C and limited the density of cesium neutrals to well below 10^7 cm^{-3} on a vapor pressure basis. The peak plasma density was varied from about 10^9 cm^{-3} to 10^{11} cm^{-3}, whereas the typical operating pressures were in the low 10^{-7} Torr range after several hours of operation. Thus the target-to-background density ratio was around unity. Typical signal-to-background ratios, determined from the beam detectors, were approximately 2 at the higher densities, consistent with the ratios determined by the plasma density and the background pressure. This compares favorably with the signal-to-background ratio for the crossed beam experiments of approximately 0.03.

The plasma density was controlled with the hot-plate bombardment power, which determined the hot-plate temperature and hence the electron emission on which the plasma density critically depends. The plasma density was measured with a Langmuir probe capable of being swept radially across the plasma column in order to determine the radial plasma line density. Plasma density profiles were taken by fixing the bias to the probe at -10 volts with respect to the hot plate and collecting the ion saturation current. The probe was moved radially

across the plasma column by a motor driven assembly and data was taken every 100 ms. A typical plasma density profile is shown in Fig. 3.

Other measurements, with the probe position fixed and the probe bias varied from -10 to +10 volts, yielded the electron temperature and the plasma potential. With these parameters and the Laframboise theory[13-15] of current collection to a probe, we were able to calculate the plasma density from the ion saturation current collected by the probe. On the basis of experimental results from other groups it is believed that this analysis is accurate to within ± 30 percent in determining the absolute value of the plasma density.[16,17] The uncertainty in the line density is the major source of systematic error in the experiment.

When beam data were being taken the probe position was fixed at the peak in the plasma density, and the ion saturation current was collected for the beam data collection time to yield a one-point determination of the plasma density. This was compared with the integrated plasma radial line density (Fig. 3) and resulted in a conversion factor between the plasma density measured at one point and the integrated radial line density. Measurements over many runs indicated that this method was accurate to within ± 13 percent.

It should be noted that the plasma target contained electrons, a possible "contaminant." However the electron thermal energy in the laboratory frame was approximately 0.25 eV, and the electron energy in the frame of the projectile cesium ion for stationary electrons in the lab frame was approximately 1.06 eV. Thus the electron energy was significantly below the threshold for ionization of the Cs^+ ion (25.1 eV), and the electrons in the target could not produce Cs^{++}.

The plasma was chopped mechanically to separate background effects from plasma effects. The chopper consisted of a rotating offset disk driven by a motor. Cams located on the drive shaft determined the chopper orientation, and micro switches were used to gate the electronic counters when the plasma was completely on or completely off. No data were accumulated when the plasma was partially on or off.

C. Beam Analysis

The target and analysis chambers are shown in Fig. 4. The beam detection system consisted of a magnetically suppressed Faraday cup for measuring Cs^+ beam currents and a secondary emission detector (SED) for detecting Cs^{++} ions. The detectors were mounted on a shaft which allowed the array to be raised or lowered to center the beams on the detectors. The Faraday cup was mounted below the secondary emission detector, and the separation of the detectors was set to be consistent with the dispersion of the Cs^+ and Cs^{++} beams due to the magnetic field of the plasma target. The Faraday cup was checked for uniformity of response and suppression of secondary electrons.

A secondary emission detector was used to measure Cs^{++} currents since the plasma target was not thick enough to produce enough current to be detectable with a Faraday cup. The detector had a 2.54-cm-diameter circular aperture and was operated in a particle counting mode. A microchannel plate amplified the charge pulses which were subsequently detected with standard pulse counting techniques. The detector was based on a design by Rinn et al.[18].

The absolute overall SED efficiency was determined in a series of measurements. A Faraday cup with a 0.01-mm-wide horizontal slit in the

back end was placed in front of the secondary emission detector and a Cs^+ beam was used to measure detector counts versus incident beam current to the Faraday cup. The circular beam was swept across the slit by electrostatic steering plates. It was assumed that the detector was at least as efficient in detecting Cs^{++} as it was in detecting Cs^+. This is reasonable on the basis of the ionization potentials of Cs^+ and Cs^{++} since the secondary electron yield is dependent on the projectile ionization potential in this velocity range.[19] The current density of the beam was shown to be uniform, and the measured detector efficiency versus count rate is shown in Fig. 5. All subsequent experiments were performed with count rates to the secondary emission detector below 10^4 counts/sec to ensure 100 percent detector efficiency. The detector also was checked for uniformity of response over the aperture; it was found to be flat.

D. System Checks

To check the transmission efficiency of the overall system and to check the collection efficiency of the secondary emission detector, a movable gas cell was designed to simulate the collision region of the plasma. Xenon was chosen as the working gas since the value of σ_{12} ($Cs^+ \rightarrow Cs^{++}$) was known from other experiments[9-11], and because of its electronic similarity to Cs^+.

The geometrical length of the cell was 5 cm, corresponding to the diameter of the plasma. It was attached to a 19-mm-diam tube which was welded to a flange such that a capacitance manometer and a gas inlet connector could be attached to the tube. A small tube ran from the gas inlet connector to the bottom of the large tube near the gas cell

to ensure that the gas cell and capacitance manometer were at the same pressure when the gas flow was steady. That is, no conductance corrections had to be made.

The large diameter tube was mounted to a movable vacuum seal which allowed vertical motion and rotation of the gas cell. The flange with the vacuum seal was connected to the plasma vacuum chamber with a stainless steel bellows; the gas cell could be tilted with four adjustment rods to align it with the beam trajectory in the magnetic field.

Alignment of the gas cell could not be done optically since the beam traveled along a curved path. Therefore, all gas-cell alignments were done by monitoring the incident ion beam current with the Faraday cup in the analysis chamber and moving the gas cell with the adjustment rods until the beam current was the same with and without the gas cell present. This was accomplished by tuning up a given energy beam and then lowering the gas cell into position. Minor adjustments of the pre-target deflection plates and the magnetic field, as well as the position of the gas cell, usually were sufficient to let all of the beam get through the cell. The entrance aperture of the gas cell was 5.08-mm diameter and the exit aperature was 6.35-mm diameter. These apertures were large enough to not interfere with the beam yet small enough to have a small conductance which allowed the gas in the cell to reach pressures measurable with the capacitance manometer.

The experiments with the movable gas cell were performed with 150 keV Cs^+ beams. Since the pressures in the target and analysis regions were too large to operate the SED in the normal mode when the gas cell was operating at the highest pressures, another way to detect Cs^{++} had to be devised. This was done by connecting all leads to the SED

together and connecting an electrometer to the emitter electrode. Thus the SED could also be operated as a Faraday cup.

The beam was swept vertically past the gas cell with the aid of the pre-target deflector plates with and without Xenon in the gas cell. The Cs^+ and Cs^{++} currents were monitored and the results are shown in Fig. 6. This showed that there was a plateau region for Cs^{++} detection which coincided with that for Cs^+ collection and confirmed the fact that the SED was large enough to collect all Cs^{++}. Secondary electron effects were responsible for the spikes near the detector edges.

As a check on the overall system, the cross section for the reaction $Cs^+ + Xe \rightarrow Cs^{++}$ was measured and compared with published results. Operating in the plateau region, the gas cell pressure was varied from zero to 5 millitorr and the Cs^{++} current was measured as a functon of gas cell pressure. The fraction of the incident beam converted to Cs^{++} was computed from the equation

$$F^{++} = \frac{I_{Cs^{++}}/2}{I_{Cs^+(p=0)}} \tag{1}$$

where $I_{Cs^+(p=0)}$ is the incident beam current measured with zero gas pressure in the gas cell. The beam current was measured frequently to confirm that the incident beam intensity was constant. The results are shown in Fig. 7. The slope of the line yields the cross section, σ_{12}. The value measured by the present method agreed to within approximately 20 percent of the value measured by Tanis et al.[9] and within 10 percent of the results subsequently reported by Neill et al.[5]

Final operating parameters for each energy were determined by tuning up the beam with the gas cell in place. Thus there was a unique set of

tune parameters (magnetic field, deflector voltage) for each energy. This ensured that the beam traversed the plasma on the same trajectory for each energy.

The half angle acceptance of the SED was measured to be 1.5° in the laboratory frame. It is believed that this angle was sufficient for energies greater than or equal to 150 keV (75 keV in the center-of-mass frame), since there was no appreciable difference between the measurements of σ_{12} in Xe for these gas cell experiments and the results from Tanis et al.[9] However, at lower energies the acceptance angle may have limited the collection efficiency. It is difficult to estimate the effects of acceptance angle without detailed differential-cross-section measurements. Trajectory calculations were performed on a computer to analyze the effects of scattering, target size and magnetic field on the effective angular acceptance of the detectors. These calculations showed that the effective angular acceptance was reduced to 1.2° from the 1.5° determined from the above geometrical consideration. Recently Neill et al.[5] have measured σ_{12} in Xe for similar reasons in their studies of Cs^++Cs^+ collisions. These results are used in the next section to provide additional estimates of the cross section error for the measured points below 75 keV.

E. Cs^+ - Cs^+ Experiment

The Cs^++Cs^+ experiments were performed after the series of Cs^++Xe gas-cell experiments. The procedure began by tuning the desired energy beam onto the Faraday cup. The plasma was turned on and usually took approximately one hour to stabilize and outgas to a

pressure in the mid to high 10^{-7} Torr range. The magnetic field and pre-target deflection voltages were set to the appropriate operating points. Beam data were taken in 30-sec intervals during which the plasma was gated on and off by the chopper. The SED detector counts and plasma ON and OFF time, as well as the incident beam current and total time were collected with scalers. The F^{++} fraction was computed by subtracting the background counts from the plasma-on data. A typical plot of F^{++} vs plasma target thickness is shown in Fig. 8. The results show a linear increase of F^{++} with plasma target thickness, consistent with single particle collision conditions. The slope of this line was determined by a least squares fit and yielded σ_{12}, the cross section for electron loss in $Cs^{+} + Cs^{+}$ collisions.

The beam was swept across the plasma to confirm the operating points (magnetic field, deflector voltage) for each measurement. Figure 9 shows a plot of the relative cross section versus deflector voltage for a 160 keV Cs^{+} beam. The plot shows a reasonable plateau. If trajectories along chords of the plasma are taken into account, then the plateau is even better. This lends further support to the adequacy of the detector acceptance angle in this energy range. Beam sweeps at lower energies were performed, but the combination of lower plasma densities (due to lower magnetic fields) and lower cross sections gave poor signal-to-noise ratios and less clear cut evidence of a plateau. However data were taken at the lower energies by operating at the properly scaled steering parameters. The added uncertainty in the low energy results is discussed in the next section.

Table 1. Summary of results for Cs^{++} production in $Cs^{+}+Cs^{+}$ collisions.

Relative standard errors are indicated. There is an additional absolute uncertainty of ± 30 percent.

Center-of-Mass Energy (keV)	σ_{12} $(10^{-16}$ cm$)^2$
50	.47 + 0.22/-0.11
60	.67 + 0.14/-0.09
70	.95 ± 0.09
75	1.38 ± 0.14
80	1.37 ± 0.10
90	1.57 ± 0.14
100	1.82 ± 0.17
110	1.87 ± 0.18

III. Results and Discussion

The cross section results for Cs^{++} formation in Cs^{+} + Cs^{+} collisions are tabulated in Table 1 and plotted in Fig. 10. The relative standard errors quoted for center-of-mass energies above and including 70 keV are based on the uncertainties described in Sec. II; that is, the ±13 percent uncertainty in plasma line density was added in quadrature to the least square fit error in the slope determination to arrive at the final relative uncertainty in the cross section for a particular run. The results in Table 1 were obtained by computing the weighted averages of the results for all runs at the same energy; between two and four measurements were made at each energy. There is an additional absolute error of 30 percent assumed for all points due to the absolute determination of the plasma density by the Langmuir-probe techniques.

Also shown in Fig. 10 are the results of others. Considerable disagreement is apparent for energies below 70 keV between the two measurements done by the crossed beam technique. It has been claimed that large angle scattering may be responsible for much of the discrepancy.[5] We have used the scattering results for Cs^+ + Xe reported by Neill et al.[5] to calculate an additional uncertainty in our results below 70 keV. Since Xe is isoelectronic with Cs^+, it is expected that the angular scattering in Cs^+ + Cs^+ collisions is similar to Cs^+ + Xe collisions. Also, since angular scattering can only reduce the apparent cross sections, the present results have an added upward uncertainty only, due to this effect. Since the effective half-angle acceptance angle for this experiment was 1.2°, the results at 50 and 60 keV (center of mass) have added uncertainties of + 22 percent and + 7 percent, respectively. Thus the reported value for σ_{12} at 60 keV is $(0.67^{+0.14}_{-0.09}) \times 10^{-16}$ cm^2 and at 50 keV the result is $(0.47^{+0.22}_{-0.11}) \times 10^{-16}$ cm^2.

The present data are in good agreement with the results of Peart et al.[3,4] but are in disagreement with the results of Dunn et al.[2] and Neill et al.[5] Large angular scattering, while possibly explaining part of the discrepancy, still does not account for all of the differences.

ACKNOWLEDGMENTS

This work was supported, in part, by a grant from the Director's Program Development Fund, Lawrence Berkeley Laboratory, and by the Director, Office of Fusion Energy, Applied Plasma Physics Division of the U.S. Department of Energy under Contract No. DE-AC03-76SF00098.

References

1. Proceedings of the Heavy Ion Fusion Workshop, Berkeley, (1979). LBL-10301.
2. K. F. Dunn, G. C. Angel, and H. B. Gilbody, J. Phys. B, 14, L623 (1979).
3. B. Peart, R. A. Forrest, and K. Dolder, J. Phys. B. 14, L383 (1981).
4. B. Peart, R. A. Forrest, and K. Dolder, J. Phys. B. 14, 1655 (1981).
5. P. A. Neill, C. G. Angel, K. F. Dunn and H. B. Gilbody, J. Phys. B, 15, 4219 (1982).
6. R. E. Olson and B. Liu, J. Phys. B. 14, L279 (1981).
7. For a more detailed description of the experiment, see K. R. Stalder, Ph.D. thesis, University of California, LBL Report 14487 (1982).
8. B. Peart, R. A. Forrest and K. Dolder, J. Phys. B. 14, L603 (1981).
9. J. A. Tanis, K. R. Stalder, J. W. Stearns and A. S. Schlachter, Bull, Am. Phys. Soc., 24, 1196 (1979).
10. I. P. Flaks, B. I. Kikiani and G. N. Ogurtsov, Sov. Phys. Tech. Phys., 10, 1590 (1966).
11. G. N. Ogurtsov, B. I. Kikiani and I. P. Flaks, Sov. Phys. Tech. Phys. 11, 362 (1966).
12. V. Laul, N. Rynn and H. Bohmer, U.C. Irvine Technical Report No. 77-29.
13. J. G. Laframboise, Univ. of Toronto, IAS, Report No. 100, (1966).
14. P. M. Chung, L. Talbot, and L. Touryan, Electric Probes in Stationary and Flowing Plasmas: Theory and Application, Springer Verlag, (1975).

15. E. W. Peterson, and L. Talbot, AIAA Journal, 8, 2215 (1979).

16. F. F. Chen, C. Etievant, and D. Mosher, Phys. Fluids, 11, 811 (1968).

17. M. Hashmi, A. J. Van der Houven Van Oordt, and J. G. Wegrove, Nuc. Fusion 8, 198 (1968).

18. K. Rinn, A. Muller, H. Eichenauer and E. Salzborn, Rev. Sci. Instrum. 53, 829 (1982).

19. F. M. J. Pichanik in Methods of Experimental Physics, Vol. 4, Part A, ed. by V. W. Hughes and H. L. Schultz, pp 348-352. Academic Press, New York, (1976).

FIGURE CAPTIONS

Figure 1. 250 kV accelerator system and experimental area.

Figure 2. Q Machine plasma-target apparatus.

Figure 3. Plasma density versus radial position. The probe bias was fixed while probe was scanned radially, and data points were taken every 100 ms. These data were analyzed according to the Laframboise theory.

Figure 4. Analysis chamber in final configuration as attached to the target chamber with bellows.

Figure 5. Count rate efficiency of the SED as a function of the incident beam current. The solid lines shows 100 efficiency at count rates below 20,000 counts/sec; the efficiency drops off at higher rates due to gain depression of the MCP.

Figure 6. Beam currents as a function of pre-target deflector voltage for the gas cell expriments.
Note plateau region for Cs^{++} and Cs^{+} currents.

Figure 7. F^{++} fraction as a function of Xe gas pressure showing linear growth of the fraction for low pressures. The measured cross section is within 20 percent of the result measured by Tanis et al.[9]

Figure 8. F^{++} fraction as a function of plasma line density for 180 keV Cs^{+} beam. Error bars shown are the typical statistical counting errors due to Poisson statistics.

Figure 9. Apparent cross section versus pre-target deflector voltage for the plasma target experiment.

Figure 10. Cross sections for Cs^{++} formation as a function of center of mass energy. Open circles: present experiment, plasma target. Also shown are the results obtained with the crossed-beam technique. Open triangles: Peart et al. (ref. 4) Open squares: Dunn et al. (ref. 2). Solid squares Neill et al. (ref. 5). Solid triangles: Peart, et al, σ_{10}. (ref. 3).

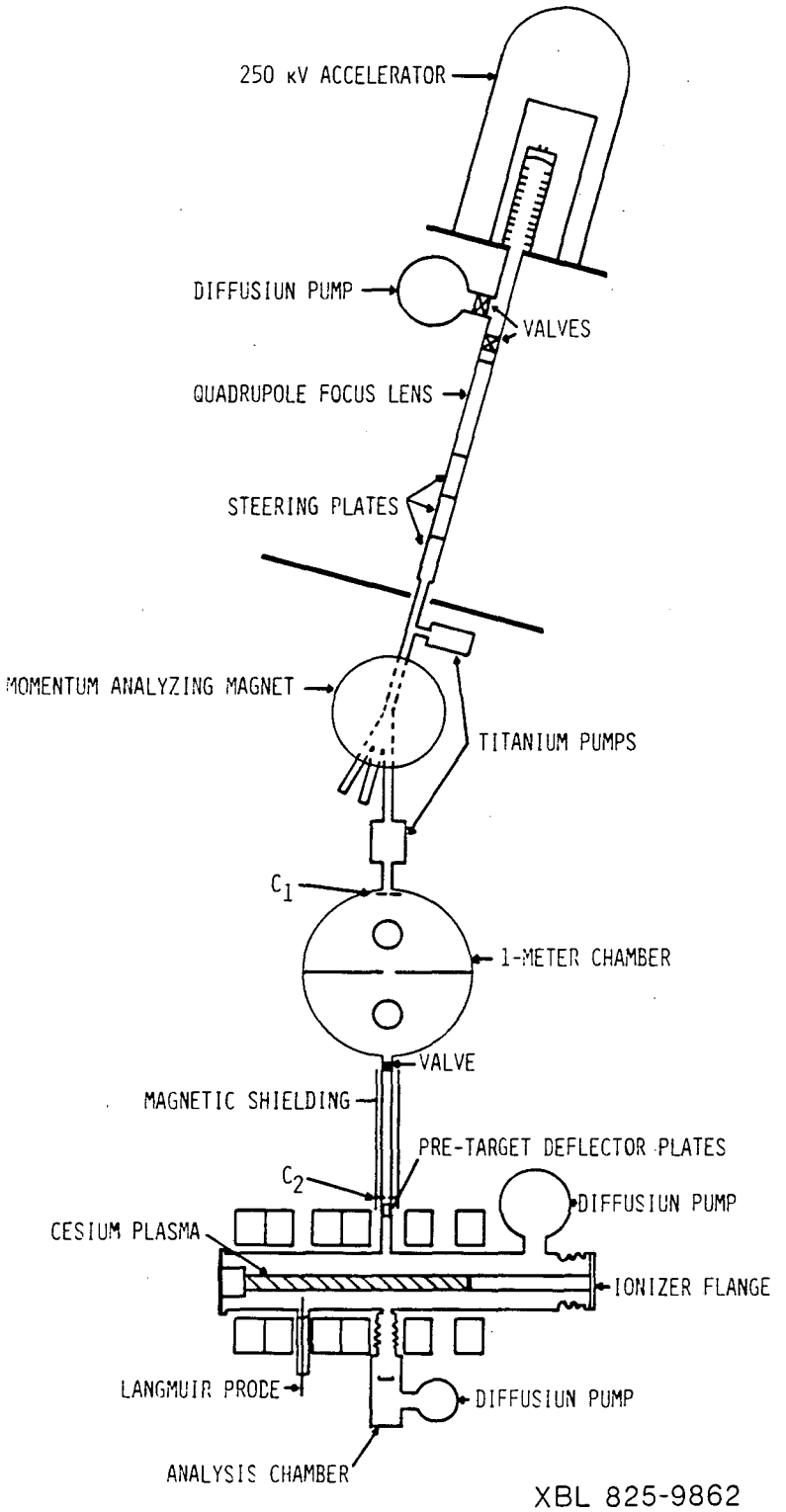
250 kV ACCELERATOR
DIFFUSIUN PUMP
VALVES
QUADRUPOLE FOCUS LENS
STEERING PLATES
MOMENTUM ANALYZING MAGNET
TITANIUM PUMPS
C_1
1-METER CHAMBER
VALVE
MAGNETIC SHIELDING
PRE-TARGET DEFLECTOR PLATES
C_2
DIFFUSIUN PUMP
CESIUM PLASMA
IONIZER FLANGE
LANGMUIR PROBE
DIFFUSIUN PUMP
ANALYSIS CHAMBER
XBL 825-9862

Figure 1

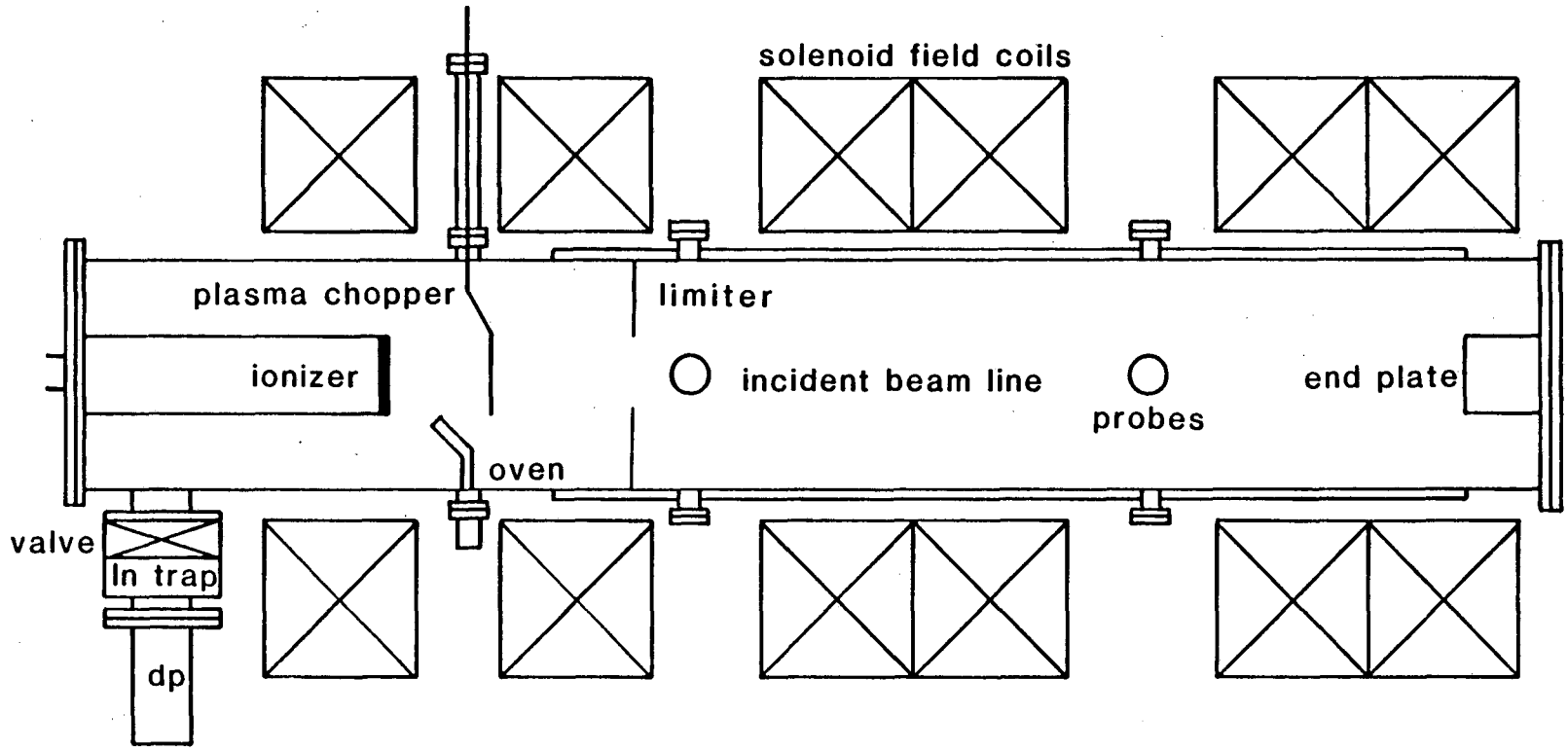

BASIC Q MACHINE GEOMETRY

XBL 825-9987

Figure 2

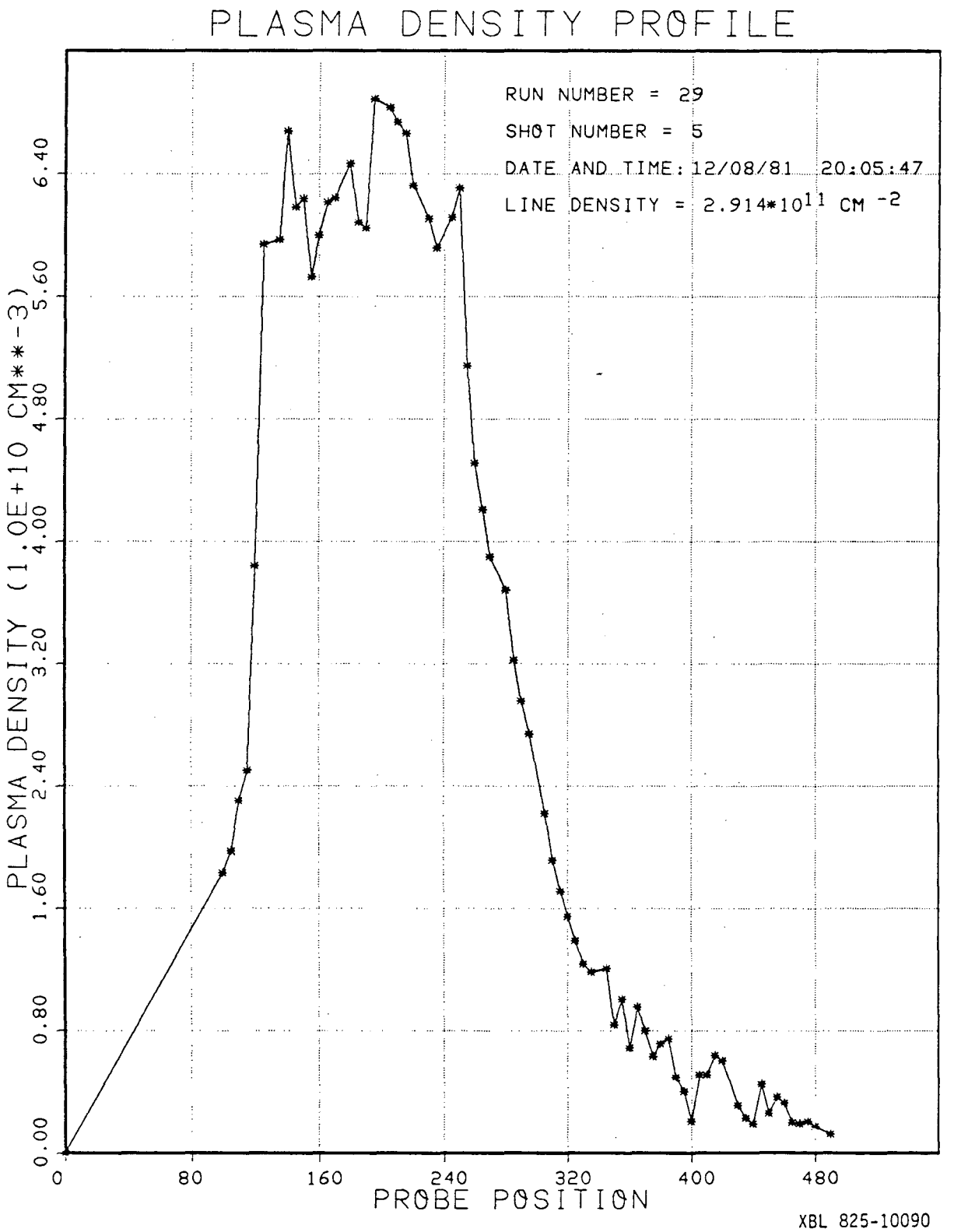
PLASMA DENSITY PROFILE
RUN NUMBER = 29
SHOT NUMBER = 5
DATE AND TIME: 12/08/81 20:05:47
LINE DENSITY = 2.914*10^11 CM -2
PLASMA DENSITY (1.0E+10 CM**-3)
0.00
0.80
1.60
2.40
3.20
4.00
4.80
5.60
6.40
0
80
160
240
320
400
480
PROBE POSITION
XBL 825-10090

Figure 3

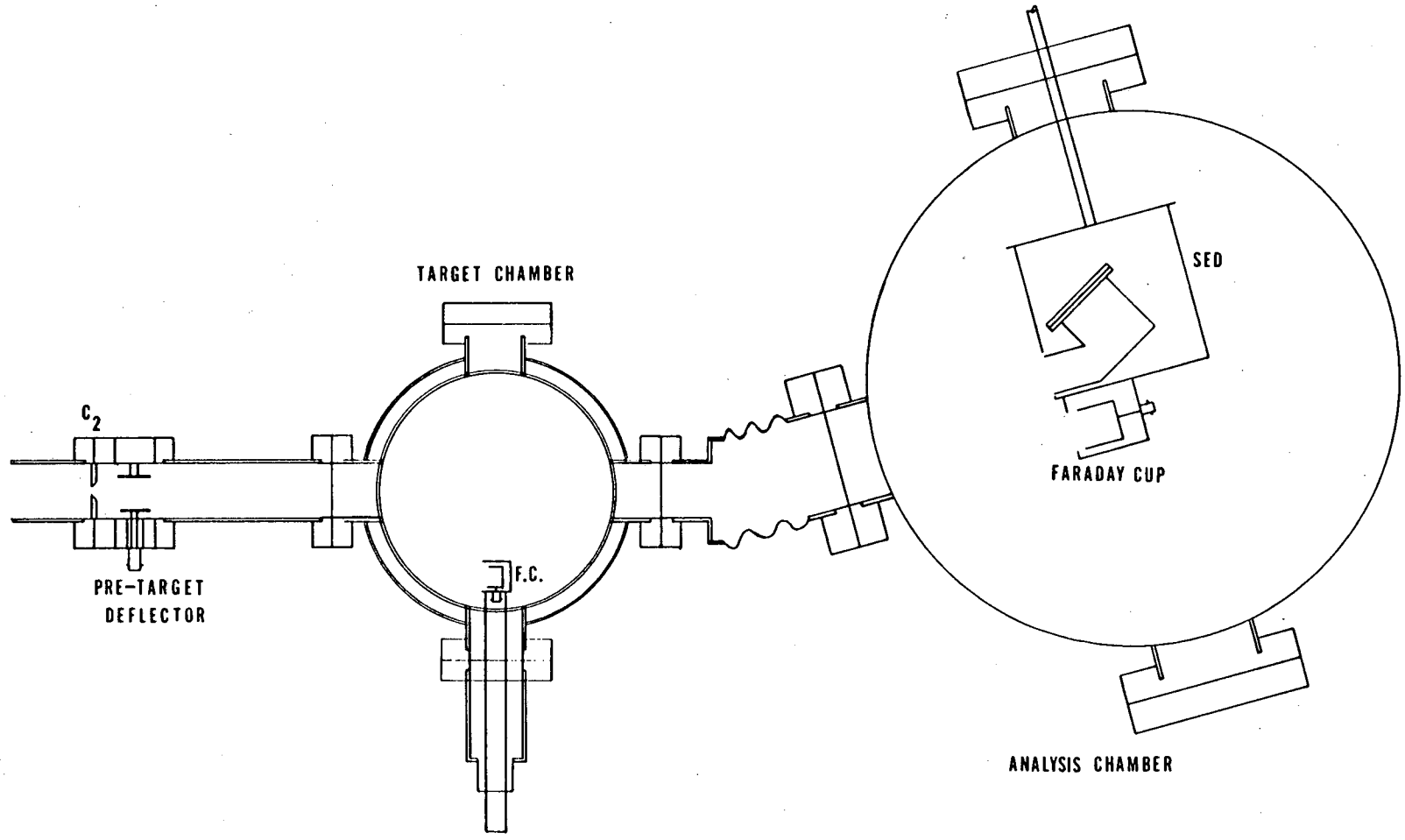

XBL 825-9989

Figure 4

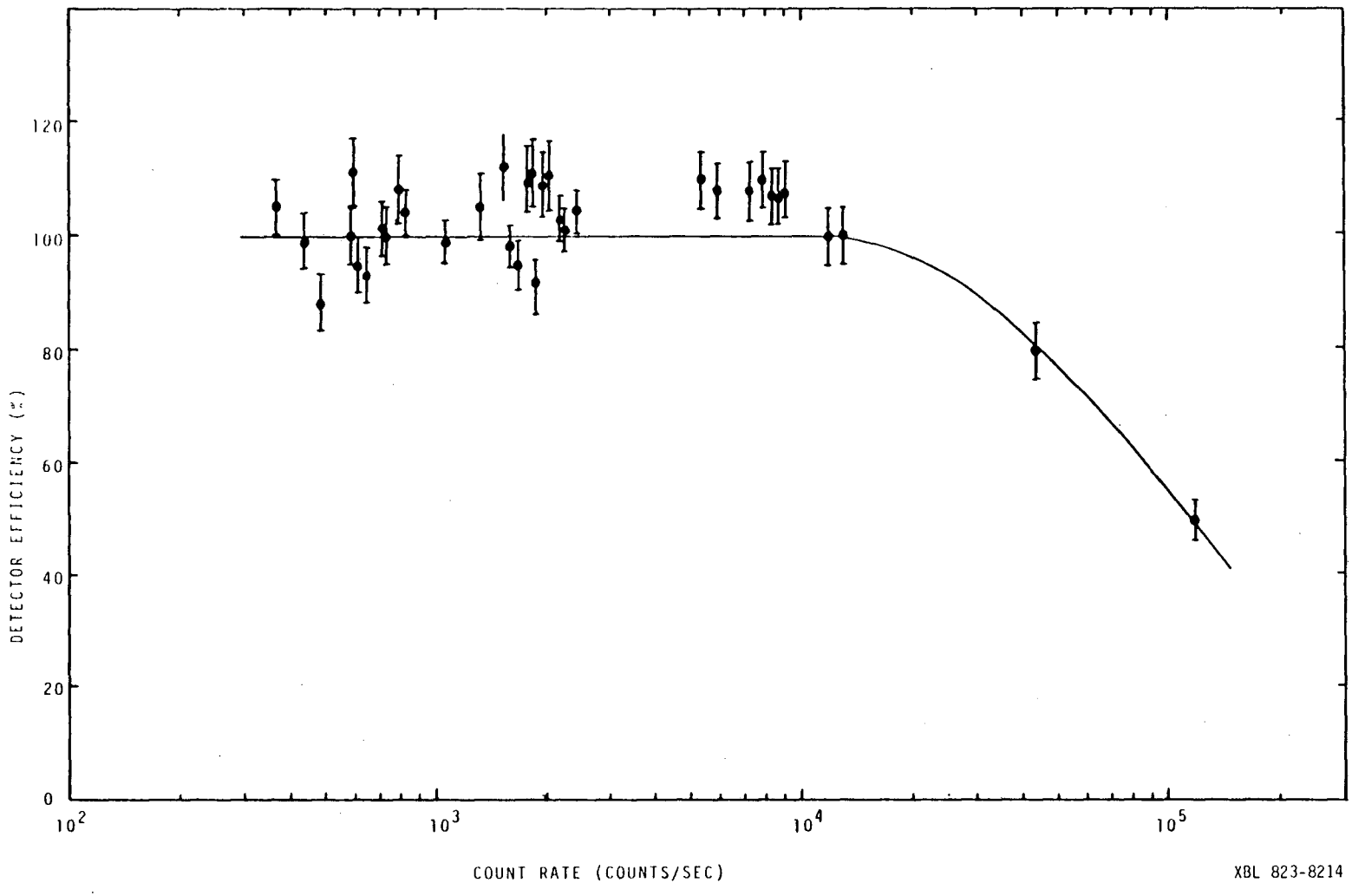
120
100
80
60
40
20
0
DETECTOR EFFICIENCY (%)
10^2
10^3
10^4
10^5
COUNT RATE (COUNTS/SEC)
XBL 823-8214

Figure 5

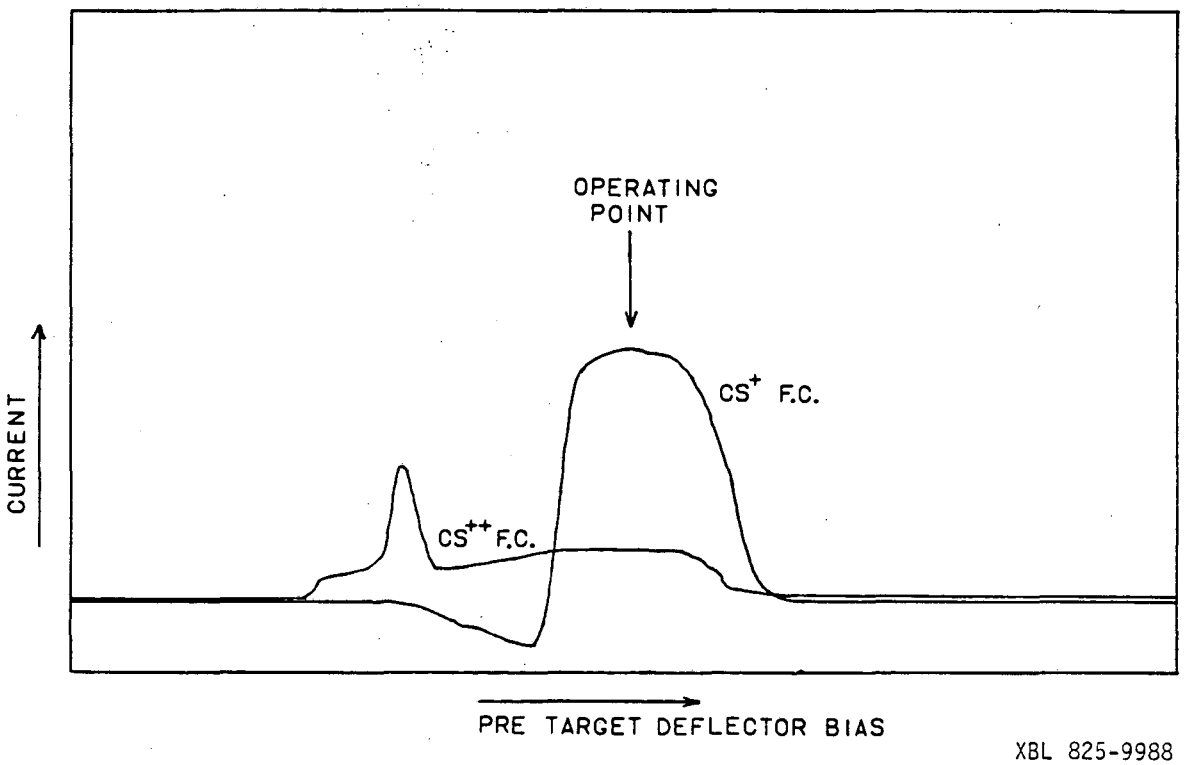
OPERATING POINT
CS+ F.C.
CS++ F.C.
CURRENT
PRE TARGET DEFLECTOR BIAS
XBL 825-9988

Figure 6

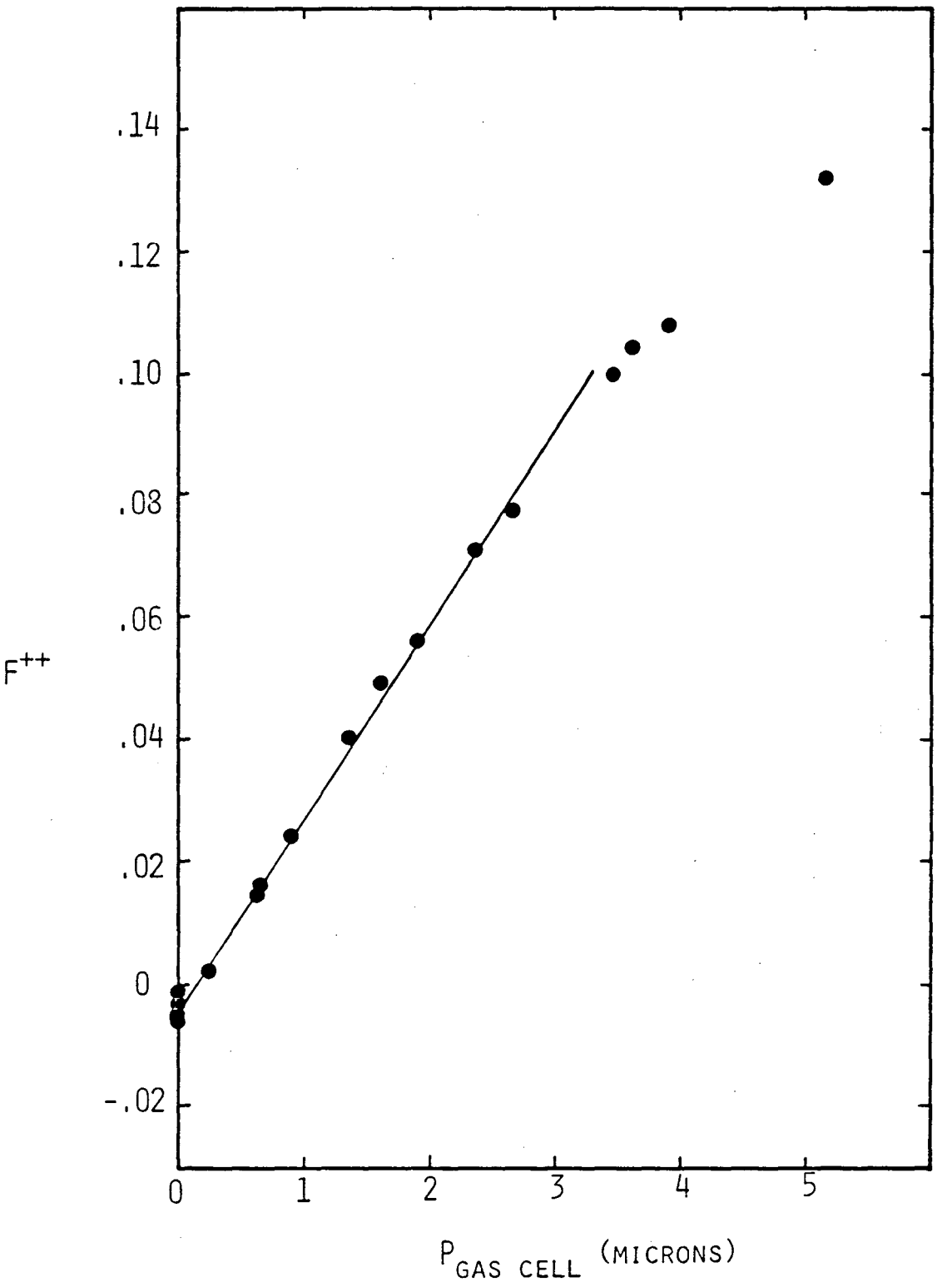

XBL 825-9866

Figure 7

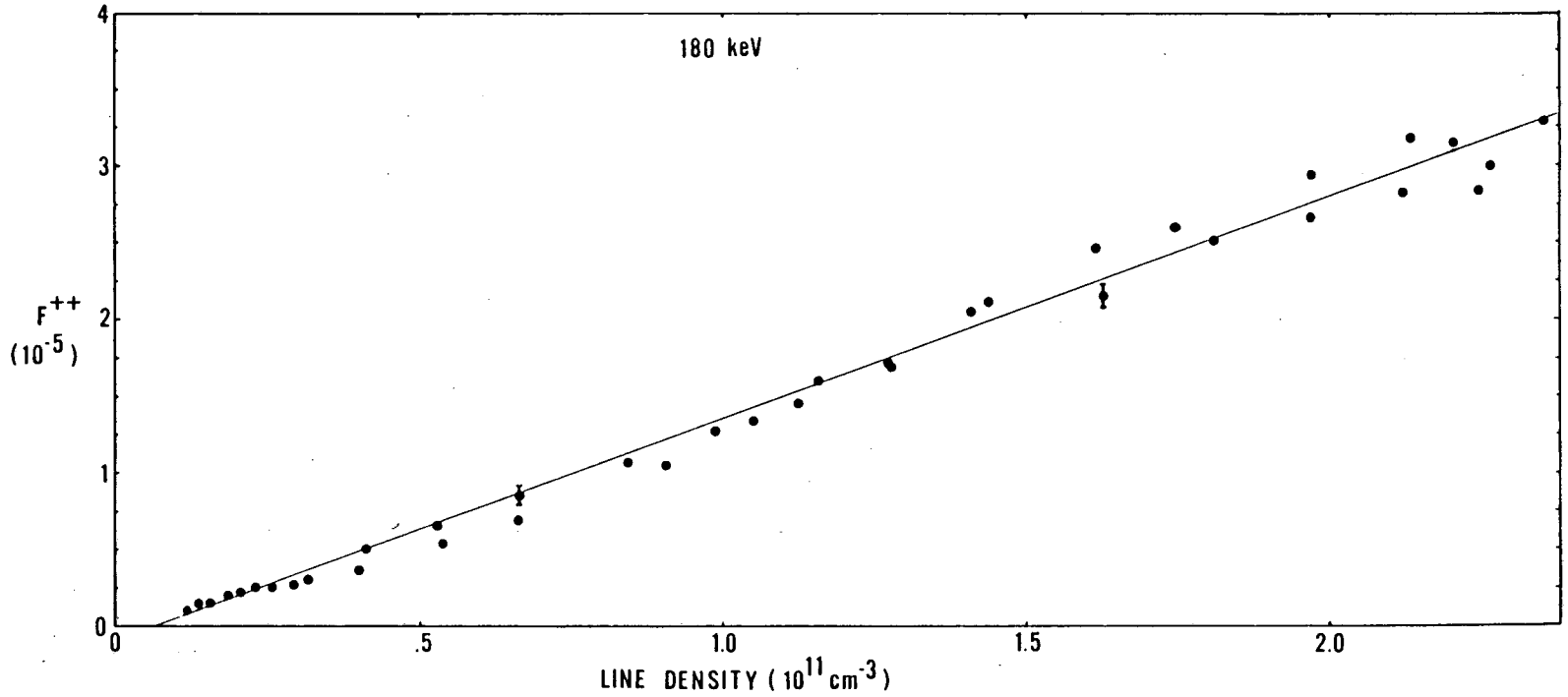

XBL 825-9859

Figure 8

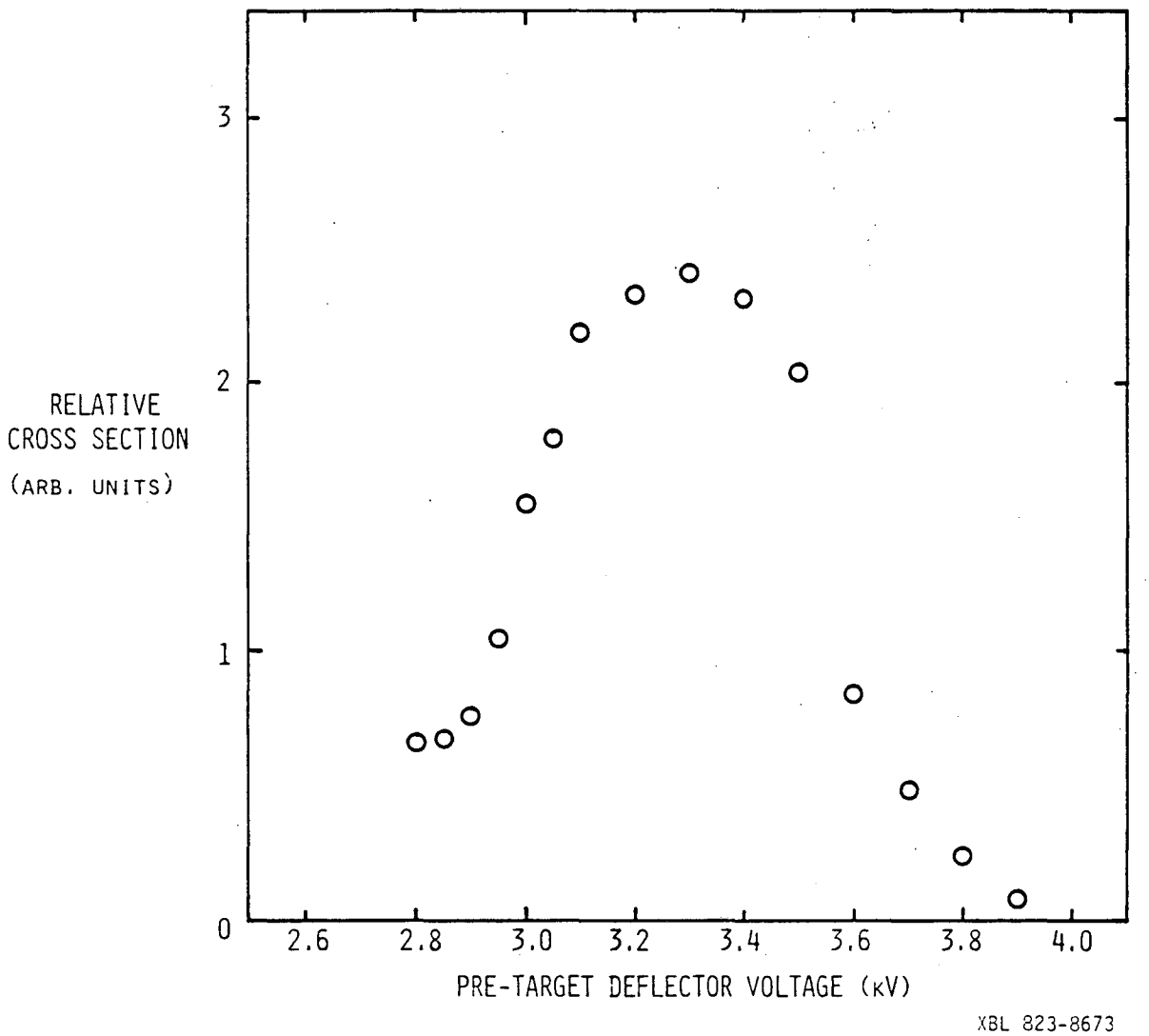
RELATIVE
CROSS SECTION
(ARB. UNITS)
0
1
2
3
2.6
2.8
3.0
3.2
3.4
3.6
3.8
4.0
PRE-TARGET DEFLECTOR VOLTAGE (kV)
XBL 823-8673

Figure 9

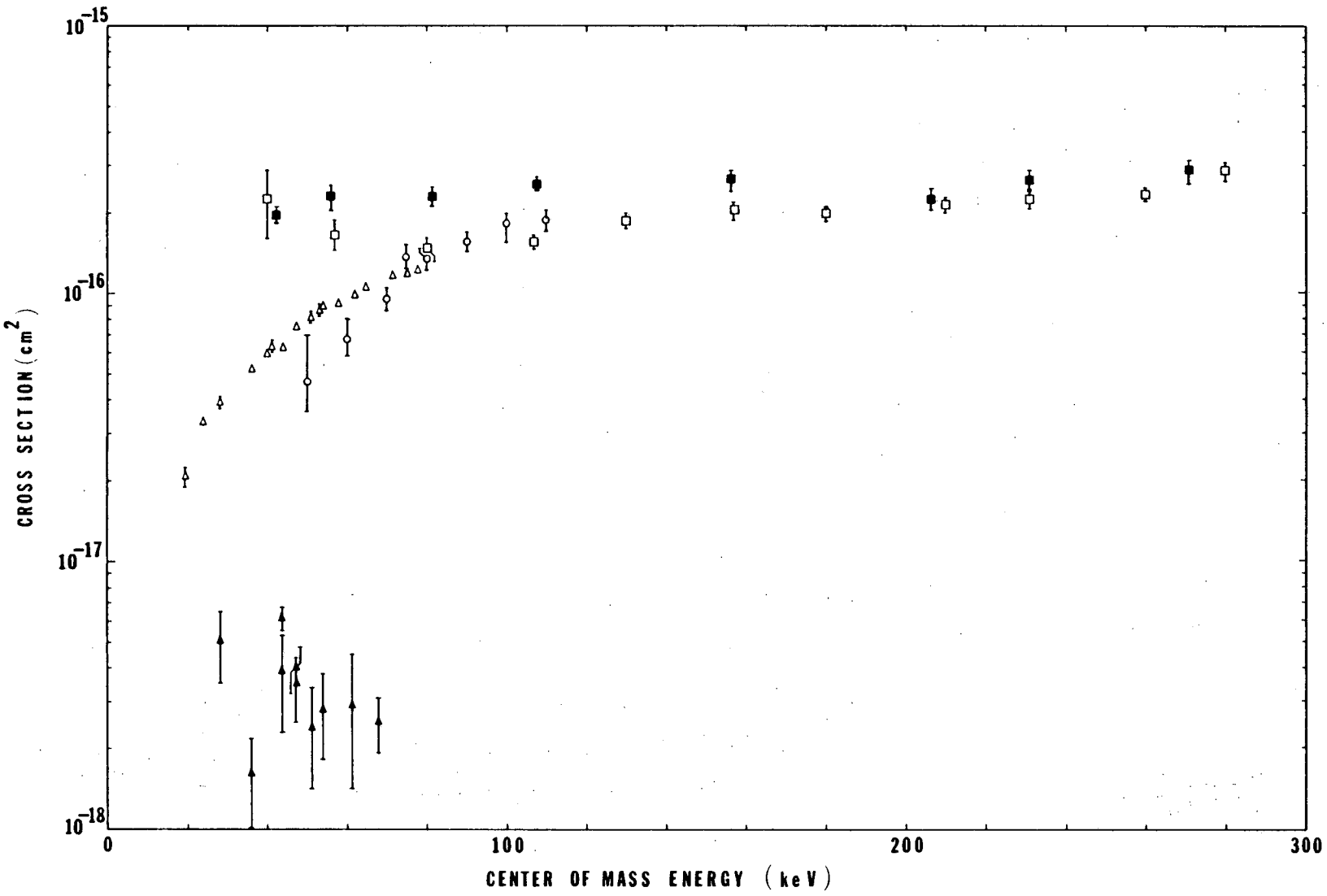

XBL 825-9861

Figure 10

This report was done with support from the Department of Energy. Any conclusions or opinions expressed in this report represent solely those of the author(s) and not necessarily those of The Regents of the University of California, the Lawrence Berkeley Laboratory or the Department of Energy.

Reference to a company or product name does not imply approval or recommendation of the product by the University of California or the U.S. Department of Energy to the exclusion of others that may be suitable.

TECHNICAL INFORMATION DEPARTMENT
LAWRENCE BERKELEY LABORATORY
UNIVERSITY OF CALIFORNIA
BERKELEY, CALIFORNIA 94720